Long-lived anionic states of H_2, HD, D_2 and T_2

Martin Čížek, Jiří Horáček*

Institute of Theoretical Physics, Charles University,

Faculty of Mathematics and Physics,

V Holešovičkách 2, Praha, Czech Republic

Wolfgang Domcke

Department of Chemistry, Technical University of Munich, D-85747 Garching, Germany

(Dated: November 23, 2006)

Abstract

A detailed investigation of the long-lived states of the hydrogen molecule anion has been performed within the *ab initio* based nonlocal resonance model. The resonances in the $X^2\Sigma_u^+$ electronic state of H_2^- are stabilised against autodetachment by molecular rotation and can be interpreted as orbiting states of H+H^- with high angular momenta ($J = 22 - 27$). The lifetimes and energies of all long-lived states have been calculated for the hydrogen molecular anion and its isotopic analogs. Recent experimental values of Heber *et al.* [Phys. Rev. A **73**, 060501(R) (2006)] for lifetimes of H_2^-, HD^- and D_2^- can be explained within the model. For T_2^-, we predict a large number of states with lifetimes up to ∼0.1 s.

*Correspondence: cizek@mbox.troja.mff.cuni.cz

I. INTRODUCTION

Recently, the existence of long-lived molecular hydrogen anions was unambiguously proven experimentally by Golser *et al.* [1]. It is clear from the time-of-flight in their apparatus that some states of negative molecular hydrogen ion must have lifetimes of the order of at least microseconds. Being the smallest molecular anion, H_2^- is also of fundamental theoretical interest.

Theoretically, the existence of a transient anionic state was assumed by many authors in the description of both e^-+H_2 [2–14] and H^-+H [15–20] collisions, because the magnitude of the inelastic cross sections requires a resonant mechanism. Early calculations of Taylor and Harris [21] indicated that the lowest $^2\Sigma_u^+$ state of H_2^- lies in the $H_2(^1\Sigma_g)$+e^- continuum. Later calculations of Bardsley, Herzenberg and Mandl [22] showed that the lifetime of the lowest p-wave shape resonance at the equilibrium internuclear distance $R = 1.4a_0$ of H_2 is of the order of 10^{-15}s. This order of magnitude of the resonance lifetime at the fixed internuclear distance has been confirmed later [23–25]. The H_2^- state becomes electronically bound for $R > 3.1a_0$ (corresponding to H+H^- at large R) but since the H+H^- interaction is attractive, the nuclei will be driven to internuclear distances smaller than $3.1a_0$. Therefore, lifetimes exceeding the vibrational period of H_2 (10^{-14}s) were not expected. While it has later been demonstrated [8, 26] that the dynamics of the metastable H_2^- collision complex cannot appropriately be described by the adiabatic autodetachment width $\Gamma(R)$ at a fixed internuclear separation R, time-dependent calculations of Gertitschke and Domcke [12], employing the nonlocal resonance model of the H_2^- dynamics, have confirmed the femtosecond timescale of the resonance decay.

Experimental evidence for existence of long-lived molecular hydrogen anions goes back to late 1950's. In 1958, Khvostenko and Dukel'skii claimed the detection of H_2^- in a mass spectrometer [27]. The observation of negative hydrogen ions from a low-energy arc source has also been reported by Hurley in 1974 [28]. Aberth *et al.* [29] confirmed the production of HD^- and D_2^- with lifetimes larger then 10μs in their plasma source. On the other hand, these ions were not found in an elaborated two-step electron-capture experiment by Bae *et al.* performed ten years later, although other known anionic species were reliably produced in the same experiment. In view of this experiment, the state of the theoretical understanding of the system as well as the possibility of contamination of the H_2^- signal by D^- (or D_2^- by

H_2D^-), the existence of long-lived, diatomic hydrogen anions remained controversial.

In 1998, we noticed that the H+H^- interaction in the lowest $^2\Sigma_u^+$ electronic state at internuclear distances $R > 3$ a_0 (where the excess electron is in a bound state) has a rather special shape, so that distinct orbiting resonances appear in H+H^- scattering for orbital angular momenta of the nuclei of $J = 22 - 26$ [20]. These resonances result from the formation of a centrifugal potential barrier at large internuclear separations ($R > 10$ a_0), arising from the combination of the centrifugal ($\sim R^{-2}$) and polarisation ($\sim R^{-4}$) terms in the potential. The existence of this barrier does not explain however, the narrow width of the resonances which is well below 1 meV, corresponding to lifetimes of $\sim 10^{-13}$s. It is a unique feature of the H_2^- potential function that for high J another barrier is formed at $R < 5$ a_0, which prevents the anion from penetration into the autodetachment region [30]. In the 1998 calculations [20], we did not pay particular attention to these resonances, since they were too weak to be experimentally discernible in the total H+H^- collision cross section. Later Xue-Feng Yang (Dalian University of Technology) has drawn our attention to the unresolved experimental controversy about the existence of long-lived molecular hydrogen anions, in connection with his experimental work [31], which indicated the formation of H_2^- in dielectric barrier discharge plasmas. We become aware of the fact that the resonances that we had calculated in H+H^- cross sections are members of a series of resonances, some of which are discernible only in e^-+H_2 collisions below the H+H^- threshold [32–34]. They are closely related to so-called boomerang oscillations in vibrational excitation cross sections [35], which are "magnified" by tunnelling through the inner barrier like in e^-+HCl scattering [36]. Our theoretical prediction for the lifetime of some of the resonances was in the order of 10^{-6}s [32]. The unambiguous detection of long-lived molecular hydrogen and deuterium anions by accelerator mass spectroscopy was subsequently published in 2005 [1]. We have reported preliminary theoretical results on the lifetimes and energies of H_2^- resonances in this paper [1]. The production of long lived H_2^- and D_2^- species was subsequently verified by Gnaser and Golser [37] using high-resolution secondary-ion mass spectrometry. They were able to separate unambiguously the D^- and H_2^- peaks in the mass spectra. Recently, the lifetimes of the H_2^-, D_2^- and HD^- species have been measured in an electrostatic ion-beam trap [38]. The measured lifetimes were 8.2 μs and 50.7 μs for H_2^- and HD^-, respectively. For D_2^-, three decay constants (23, 84 and 1890 μs) were observed [38].

In the present work, we have performed a comprehensive investigation of the energies

and lifetimes of the long-lived resonance states in H_2^-, HD^-, D_2^- and T_2^-. The underlying nonlocal resonance model for H_2^- [20] is briefly described. We have implemented a new technique which allows us to calculate efficiently and accurately the positions and widths of extremely narrow orbiting resonances.

II. BRIEF OUTLINE OF THEORY

To describe the electronic and nuclear dynamics of the H_2^- system, we use the nonlocal resonance theory reviewed in Ref. [39]. The basic model for e^-+H_2 collisions, based on projection-operator formalism of scattering theory, was constructed by Berman, Mündel and Domcke [25]. The model is based on the Fano picture of the discrete $H_2^-(^2\Sigma_u)$ state embedded in the $H_2(X^1\Sigma_g)$+e^- continuum. We have adjusted the long-range part of the H+H^- potential to treat the polarisation interaction properly [20]. Higher anionic states are not considered, since they are autodetaching at all internuclear distances and their lifetimes are expected to be very short. The only exception is the lowest state of $^2\Sigma_g$ symmetry of H_2^-, which becomes electronically stable for internuclear distances beyond about $6a_0$. However, this potential function is repulsive [50] resulting in fast dissociation to H+H^-.

A. Effective Hamiltonian for the nuclear motion within the nonlocal resonance model

The basic idea of the nonlocal resonance model is the division of the electronic Hilbert space of the problem (for each position of the nuclei) into a discrete state (ϕ_d) and an electronic continuum. The main difficulty in the description of resonant electron-molecule collisions is the failure of the Born-Oppenheimer approximation. The success of the nonlocal resonance model for the description of resonant electron-molecule collisions [40] is due to the fact that it is often possible to select ϕ_d in such a way that the requirement of the orthogonality of the continuum states ϕ_e to ϕ_d removes the shape resonance, which are responsible for the nonadiabatic coupling, from the continuum.

After the selection of the appropriate diabatic basis ϕ_e, ϕ_d, we expand the complete (electronic plus nuclear) wave function of the system in this basis

$$\Psi(R,r) = \Psi_d(R)\phi_d(R,r) + \int \mathrm{d}e\ \Psi_e(R)\phi_e(R,r), \tag{1}$$

where R stands for the nuclear coordinate and r for the electronic coordinates. Eliminating $\Psi_e(R)$, the equation of motion for the function $\Psi_d(R)$ is governed by the effective Hamiltonian

$$H_{\rm eff} = T_{\rm N} + V_d(R) + \hat{F}(E), \tag{2}$$

where $T_{\rm N} = -\frac{1}{2\mu}\Delta_R$ is the nuclear kinetic-energy operator, $V_d(R)$ is the discrete-state potential (mean value of electronic Hamiltonian in the state ϕ_d) and $\hat{F}(E)$ is the effective potential resulting from the interaction of the discrete state with the continuum, which in the nuclear coordinate representation reads

$$\langle R|\hat{F}(E)|R'\rangle = \int {\rm d}e V_{de}(R)\left[E - e - T_{\rm N} - V_0(R) + i0\right]^{-1} V^*_{de}(R'). \tag{3}$$

Here and in the following text the hat symbol indicates the nonlocality of the operator in R-representation. Here $V_0(R)$ is the potential-energy function of the neutral molecule, $V_{de}(R)$ is the coupling matrix element of the electronic Hamiltonian between ϕ_d and ϕ_e, E is the total energy of the system and e is the kinetic energy of the continuum electron. The partial-wave expansion of the nuclear wave-function (1) gives rise to the standard centrifugal term $J(J+1)/2\mu R^2$, which adds to the potentials $V_0(R)$ and $V_d(R)$. The effective Hamiltonian for the radial nuclear wave function $\Psi^J_d(R)$ thus reads [41]

$$H^J_{\rm eff} = T_{\rm N} + \frac{J(J+1)}{2\mu R^2} + V_d(R) + \hat{F}^J(E) \equiv T_{\rm N} + \hat{W}^J. \tag{4}$$

We would like to point out that we neglect here the recoil angular momentum due to electron release from the anion. In our previous work on electron collisions with H_2 as well as $H+H^-$ collisions we tested this approximation. Its effect on the cross sections and resonance widths is small [20, 30, 34]

B. Description of orbiting resonances within the nonlocal resonance model

In [1] we have shown that very narrow resonances are present in both dissociative attachment and vibrational excitation cross sections for energies close to bound states in the real part of the effective potential (2). Even knowing approximately the positions of these resonances, it is difficult to find them in the cross sections, since the width of some of them is below 10^{-6} eV. To obtain a comprehensive description of these resonances, we need an effective and reliable method to find the resonances. A direct calculation of the poles of the

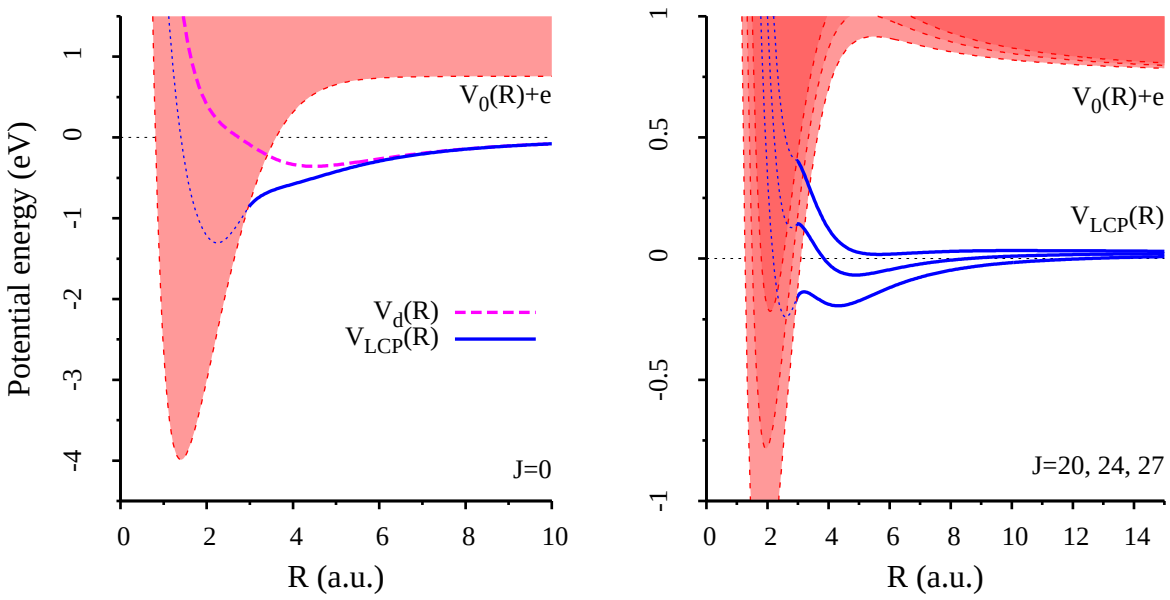

FIG. 1: (Color online) Potential-energy curves (including the centrifugal term $J(J+1)/2\mu R^2$) for angular momentum $J = 0$ (left) and $J = 20$, 24, 27 (right). The area above $V_0(R)$ (electron continuum) is shaded. $V_{LCP}(R)$ corresponds to the energy of the (electronically) bound state (solid line) or to the pole of K-matrix (dotted line).

scattering S-matrix has been performed for $J = 0$ within the local-complex-potential (LCP) approximation by Narevicius and Moiseyev [42] employing complex scaling methods. In the case of long-lived resonances for high J, it is inconvenient to use methods which are based on analytic continuation in to the complex energy plane, since even a very small relative error in the complex energy $E_R - i\Gamma/2$ would spoil the imaginary part, since $\Gamma \ll E_R$.

A convenient way to obtain the resonance energy and width directly is the use of a projection-operator method for the nuclear dynamics governed by the effective Hamiltonian (2). If we can guess a square-integrable function Φ, which approximates the resonance under consideration then the resonance energy and position can by found from [43, 44]

$$E_0 = \langle\Phi|H_{\rm eff}(E_0)|\Phi\rangle + \langle\Phi|H_{\rm eff}(E_0)\bar{G}(E_0)H_{\rm eff}(E_0)|\Phi\rangle, \tag{5}$$

where $\bar{G}(E)$ is the so-called background Green's function. This equation has to be solved iteratively. The final result does not depend on the choice of Φ. For a narrow resonance and with a good choice of Φ, we can hope to obtain accurate result even with a single iteration [43]. In our previous attempts to characterise the resonances in the vibrational excitation

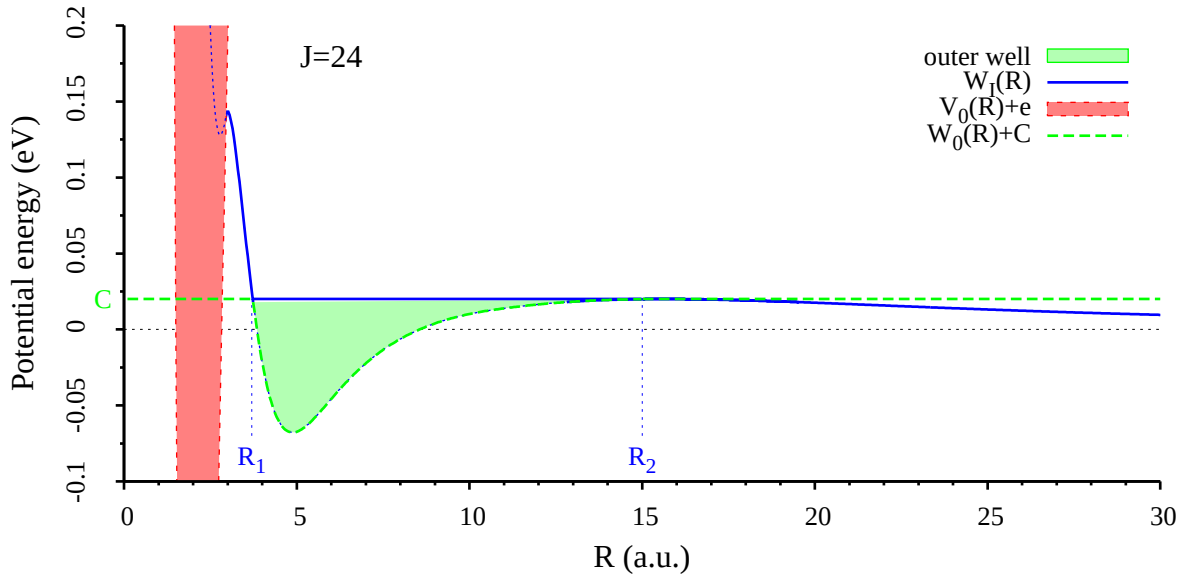

FIG. 2: (Color online) Decomposition of $V_{\rm LCP}$ into W_0 (dashed line with shaded well) and W_I (solid line). The autodetachment region (decay into the electron continuum) is indicated by the dark shaded area.

cross sections [1, 30, 34] we found good agreement between the positions of resonances and the energies of bound states in the local effective potential. Within this approximation, the full nonlocal interaction $\hat{W}^J$ is replaced by the energy-independent complex potential energy function $V_{\rm LCP}(R) - i/2\Gamma_{\rm LCP}(R)$. This potential can directly be calculated from the functions $V_0(R)$, $V_d(R)$ and $V_{de}(R)$ defining the nonlocal resonance model [20, 39]. For $R \gtrsim 3a_0$, $V_{\rm LCP}(R)$ is real and coincides with the adiabatic potential for the ground electronic state of the molecular anion at fixed R. The potentials $V_0(R)$, $V_d(R)$ and $V_{\rm LCP}(R)$ are shown in Fig. 1 for $J = 0$ (left) and for rotating molecules with $J = 20, 24, 27$ (right). The formation of the outer well and the barrier separating it from the inner autodetachment region ($R < 3a_0$) is clearly seen.

Generalising the method of Gurwitz [43], we decompose the potential $V_{\rm LCP}(R)$ into potential well $W_0(R)$ and the residual interaction $W_I(R)$,

$$V_{\rm LCP}(R) = W_0(R) + W_I(R) \tag{6}$$

where

$$W_0(R) \;=\; V_{\rm LCP}(R) - C \qquad \text{for } R_1 < R < R_2,$$

$$
\begin{aligned}
W_0(R) &= 0 \qquad \text{elsewhere,} \\
W_I(R) &= C \qquad \text{for } R_1 < R < R_2, \\
W_0(R) &= V_{\mathrm{LCP}}(R) \qquad \text{elsewhere.}
\end{aligned}
$$

Here R_1 and R_2 define the outer-well region and $C = W_{\mathrm{LCP}}(R_1) = W_{\mathrm{LCP}}(R_2)$. As an example, we show the decomposition of the potential for $J = 24$ in Fig. 2.

The complete effective interaction $\hat{W}^J(R)$ is then written in the form

$$
\hat{W}^J = W_0(R) + W_I(R) + (\hat{W}^J - V_{\mathrm{LCP}}(R)) \equiv W_0(R) + \overline{W}. \tag{7}
$$

The bound states Φ_n^J in the potential W_0 are a convenient choice for Φ. Equation (5) for the position of the resonances now reads

$$
E_0 = E_n^J + \langle \Phi_n^J | \overline{W}(E_0) | \Phi_n^J \rangle + \langle \Phi_n^J | \overline{W}(E_0) \overline{G}(E_0) \overline{W}(E_0) | \Phi_n^J \rangle, \tag{8}
$$

where we have utilised the orthogonality of the nuclear background continuum to Φ. The expression (8) is readily evaluated, since the Green's function element can be calculated with the methods which have been developed for the evaluation of the vibrational excitation cross sections [34].

Equation (8) remains valid for any separation of $H_{\mathrm{eff}} = H_0 + \overline{W}$, E_n^J and Φ_n^J being eigenenergies and eigenstates of $H_0 = T_N + W_0$. The special choice of W_0 defined above ensures that the Φ_n^J describe the states localised in the outer potential well. Furthermore, this choice allows us to overcome certain numerical difficulties. We find E_n^J and Φ_n^J by the diagonalisation of H_0 in the Fourier basis using the discrete-variable-representation (DVR) method. This procedure is numerically unstable in the classically forbidden region. The special choice of $W_0(R)$, which is constant outside the interval $[R_1, R_2]$, makes it possible to replace numerically inaccurate values of $\Phi_n^J(R)$ by analytical solutions in the classically forbidden region.

We tested this method for the positions and widths of H_2^- resonances obtained from vibrational excitation and dissociative attachment cross sections [30, 34] by fitting the resonance peaks to Fano line shapes. The procedure was then straightforwardly used for the other isotopes.

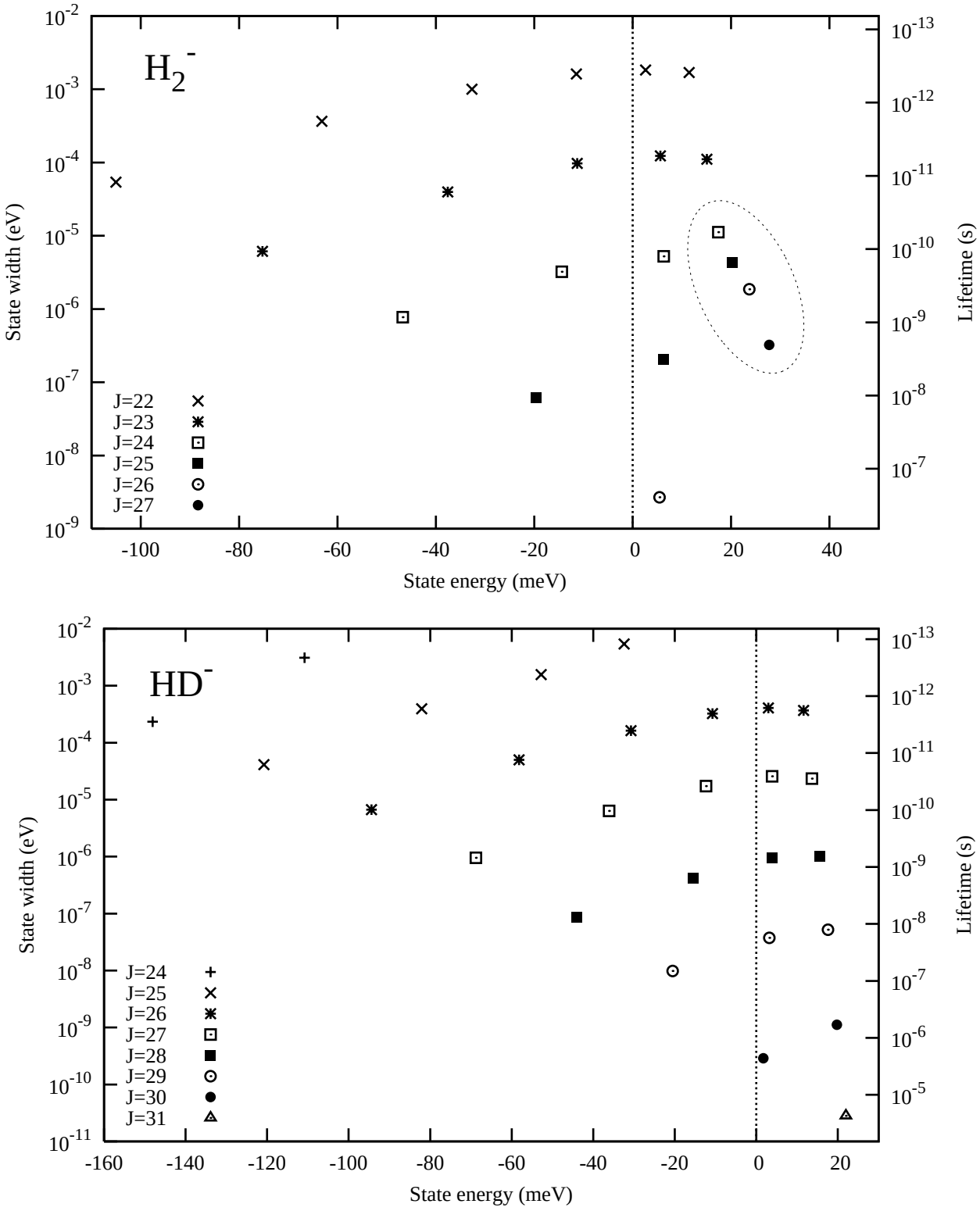

FIG. 3: Summary of the energies and decay widths/lifetimes of narrow resonances in H_2^- and HD^-. Energies are given relative to the H+H$^-$ threshold. The resonances with high dissociation rates are encircled.

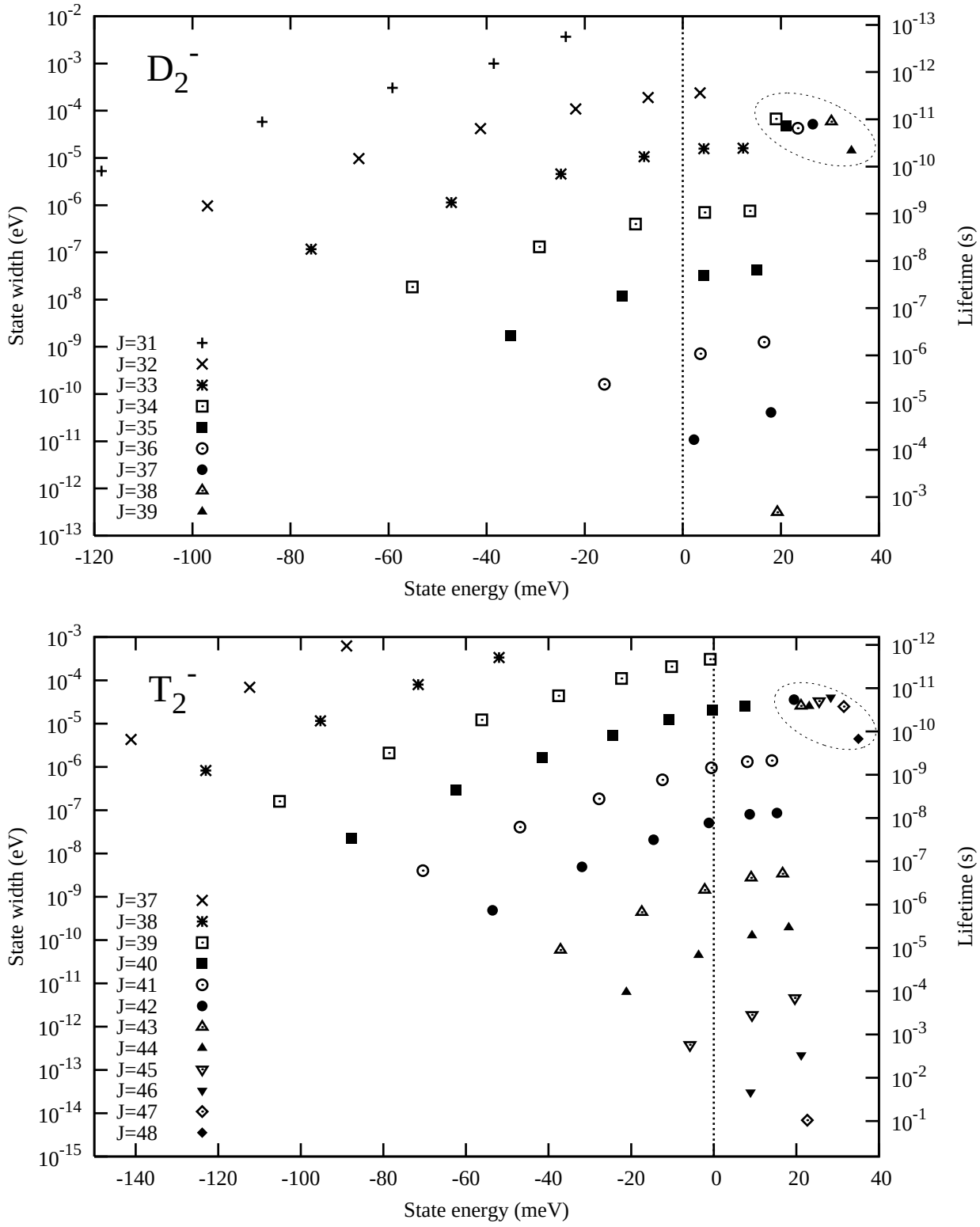

FIG. 4: Summary of the energies and decay widths/lifetimes of narrow resonances in D_2^- and T_2^-. The resonances with high dissociation rates are encircled.

III. RESULTS: ENERGIES AND LIFETIMES

An overview of all narrow resonances of H_2^-, calculated as described above, is given in Fig. 3 (top), where we have plotted the resonance lifetime against the energy. The energy scale is defined such that $E = 0$ corresponds to the H+H$^-$ dissociation threshold. The resonances with $E > 0$ thus can decay both into the autodetachment ($H_2 + e^-$) and dissociation (H+H$^-$) channels. Autodetachment is the only decay channel for the resonances with $E < 0$. The resonance lifetime is given on the right side of the figure.

For each J we observe a series of resonances. The characteristic features of the plot can be understood in terms of the shape of the adiabatic potentials (see Fig. 1). For fixed J, the width of the resonances grows with energy as expected for the quantum tunnelling effect. For $J = 22, 23$, the trend is violated for the highest resonances, which are located above the inner barrier. Their wave functions extend into the autodetachment region and these resonances develop into boomerang oscillations. The additional narrowing can be understood as an interference effect [34] or the interaction of many overlapping resonances [42]. For higher J, such resonances do not exist, since the inner barrier is always higher than the outer barrier.

The decrease of the width and increase of the energy with increasing J is associated with the increase of the inner barrier and the bottom of the well, respectively. In addition, the width is decreasing with J due to the increasing energy of the final states $H_2(J, v)$, which decreases the number of states available for autoionisation into $H_2(J, v) + e^-$. The sharp decrease of the lifetimes of the highest resonances of H_2^- with large J (encircled in Fig. 3) is due to a change of the shape of the outer well with J. These resonances have very small decay rate to H_2+e$^-$ but they can decay with rather large rates into H+H$^-$ through outer barrier. For $J = 26, 27$, the outer well becomes very shallow and for $J = 28$ the outer well does not support a resonance. The outer well disappears for higher J's.

The bottom part of Fig. 3 shows the results for HD$^-$. The isotope effects are more or less trivial. The widths are smaller for the heavier system since it is more difficult for the heavier particles to tunnel through the barriers. The resonances are more closely spaced in energy. The shape of the effective potential is determined by the centrifugal term $J(J + 1)/2\mu R^2$. For the heavier systems we thus expect to get a similar shape of the potential for larger J (J scales approximately as $\sqrt{\mu}$). The angular momenta of the resonances of HD$^-$ are thus generally larger than those of H_2^-. The most conspicuous qualitative difference from H_2^- is the

absence of the resonances with high J and enhanced dissociation rate. The reason for their absence is as follows. For HD^-, the highest narrow resonance for each J is still significantly below the outer barrier, while the next resonance lies already above the barrier. In H_2^-, on the other hand, the resonances lie just few meV below the top of the outer barrier. This causes smaller lifetimes and renders them quite sensitive to small changes in the potential.

The data for D_2^- and T_2^- are given in Fig. 4. The density of states and the lifetimes increase with the mass, as expected. The lifetimes reach 2 ms and 0.1 s for D_2^- and T_2^- respectively. Unlike for HD^-, resonances with a high dissociation rate exist and are grouped in the top right corner of the plots.

IV. COMPARISON WITH THE EXPERIMENTAL DATA

Very recently, the lifetimes of H_2^- and its isotopic analogs created by sputtering were measured in an electrostatic ion beam trap in the Weizmann institute [38]. In this apparatus, metastable ions with lifetimes of at least $\sim \mu$s can be detected. The lifetimes measured in [38] from the trap-loss rates are collected in Table I together with the results of the present calculations.

We observe a nice agreement for the lifetimes of the three states observed in D_2^-[51]. For HD^-, the difference between theory and experiment is about a factor of 2. For H_2^-, on the other hand, the longest calculated lifetime (0.25 μs) is more than one order of magnitude smaller than the measured one.

To understand the possible origin of these discrepancies, we tested the sensitivity of the resonance positions and lifetimes with respect to small changes in the effective nuclear potential. As a test, we have slightly deepened the outer potential well by adding the term $E_T \exp[-(R-6)^2]$ to the discrete-state potential $V_d(R)$. The energies and lifetimes obtained for $E_T = -10$meV of are given in parentheses in Table I. We observe that the energies are shifted down by 3-7 meV and that changes in the lifetime by a factor of 2 are easily possible. Furthermore, the lifetimes of the resonances with a high dissociation rate are extremely sensitive to the position of their energy relative to the top of the outer potential barrier. These resonances are not included in Table I, since their lifetimes are not that large, with the exception of the $(J, v) = (27, 0)$ resonance in H_2^-. The lifetime of this resonance changed by three orders of magnitude (from 2 ns to 6 μs) as a consequence of the small change in

	J	v	E	τ (Theory)	τ (Experiment)
H_2^-	26	0	5 (-1)	0.25 (0.38)	8.2±1.5
	27	0	28 (22)	0.002 (6.3)	
HD^-	31	0	22 (15)	23 (49)	50.7±1
	30	0	1.7 (-5)	2 (4)	
	30	1	20 (17)	0.6 (0.8)	
D_2^-	38	0	19 (12)	2108 (3900)	1890±80
	37	0	2 (-5)	61 (140)	84±3
	37	1	18 (15)	16 (17)	23±3
	36	0	-16 (-22)	4 (9)	
	36	1	4 (0)	0.9 (1.1)	
	36	2	17 (15)	0.5 (0.5)	

	J	v	E	τ (Theory)
T_2^-	47	0	23	96ms
	46	0	9	21ms
	46	1	21	3ms
	45	0	-6	2ms
	45	1	9	350
	45	2	20	140
	44	0	-21	105
	44	1	-4	15
	44	2	9	5
	44	3	18	3
	43	0	-37	11
	43	1	-17	1
	42	0	-53	1

TABLE I: Theoretical and experimental results for resonances with lifetimes in the μs to ms range. The quantum numbers J and v are given for each resonance. The lifetimes τ are given in μs (unless stated otherwise). The energies E of each resonance relative to the dissociation threshold are given in meV. The numbers in parentheses illustrate the sensitivity of the energies and lifetimes with respect to changes in the potential (see text).

the potential energy. The lifetime obtained with the modified potential is very close to the measured value of (8.2 ± 1.5) μs. There are no such dissociating resonances for HD^-. Some dissociating resonances in D_2^- are similarly sensitive to changes in the potential, but their lifetimes are not in the μs range.

The potential-energy curve $V_d(R)$ for $R > 3a_0$ is based on data of Senekowitsch *et al.* [45] which were recently found out to be accurate within few meV [46]. The effects of correlated electron and proton motion are of similar size [46]. In addition, there are dynamic effects of the nuclear rotation on the electronic energies. Considering these limitations of the model, the calculated lifetimes are in full agreement with the measured data. We conclude, in particular, that it does not seem necessary to invoke the existence of the other electronic

states of H_2^- [38] for the explanation of the lifetimes of H_2^- and its isotopomers.

V. CONCLUSIONS

We have employed the projection-operator method to calculate the energies and lifetimes of resonances within the nonlocal resonance model for H_2^-. The method has been applied to characterise the outer-well resonances in H_2^-, HD^-, D_2^- and T_2^-. A comprehensive set of resonance energies and lifetimes has been calculated.

The predicted lifetimes generally are in qualitative agreement with experiment [38], although the calculated lifetime is too low by an order of magnitude for H_2^-. For HD^-, the deviation from experiment is within a factor of two. The calculated lifetimes of D_2^- are in good agreement with the three measured lifetimes [38].

We predict the existence of many more resonances with lifetimes below μs, down to the ps range. The detection of these short-lived species and the accurate prediction of their lifetimes represents a challenge both to experiment and theory, considering the sensitivity of the lifetimes to the internuclear potential and the autodetachment width. We have shown that the deviation from experiment can be explained by a rather small ($\sim$10 meV) modification of the *ab initio* $H+H^-$ potential. The resonances which decay primarily by dissociation into $H+H^-$ are particularly sensitive to changes in the $H+H^-$ potential. The lifetimes of the resonances which decay primarily by autodetachment are much less sensitive to details of the H_2^- potential-energy function.

Furthermore we have calculated the energies and the lifetimes of the T_2^- states. It is predicted that these resonances have lifetimes up to 0.1s.

An issue which deserves further attention is the mechanism of the creation of these metastable species under various conditions. The creation of the metastable states in binary e^-+H_2 or $H+H^-$ collisions is difficult, although cross sections at resonance exceed 200Å^2. Since the widths are of the order of $10^{-6} - 10^{-9}$ eV, the production rates with any realistic experimental energy resolution would be very small. This can explain the mixed success of the experimental efforts to detect these species [47–49]. Recent experiments [1, 37] have shown that it is possible to create metastable H_2^- species in ion collisions with hydrogen-rich surfaces. We expect that the creation of these species may be feasible in collisions involving molecular targets, like H^-+H_2. It would also be interesting to investigate the destruction

mechanism of the anions in collisions with H and H_2. A better understanding of these processes is important for the optimisation of plasma conditions for the efficient generation of H^-, D^- or T^- anions.

Acknowledgments

We would like to thank to Xue-Feng Yang (Dalian University of Technology, China) for bringing the controversy about the existence of metastable molecular hydrogen anions to our attention and to Hartmut Hotop (Technical University of Kaiserslautern) for drawing our attention the the experiments of Hubert Gnaser and Robin Golser.

This work has been supported by the Grant Agency of the Czech Republic as project no. GAČR 202/03/D112. Support from the Czech Academy of Sciences by the grant GAAV IAA400400501 and by Výzkumný záměr MSM0021620835 "Fyzika molekulárních, makromolekulárních a biologických systémů" of MŠMT is acknowledged.

---

[1] R. Golser, H. Gnaser, W. Kutschera, A. Priller, P. Steier, A. Wallner, M. Čížek, J. Horáček, and W. Domcke, Phys. Rev. Lett. **94**, 223003 (2005).

[2] Y. N. Demkov, Physics Letters **15**, 235 (1965).

[3] J. N. Bardsley, A. Herzenberg, and F. Mandl, Proc. Phys. Soc. **89**, 321 (1966).

[4] J. M. Wadehra and J. N. Bardsley, Phys. Rev. Lett. **41**, 1795 (1978).

[5] J. M. Wadehra, Appl. Phys. Lett. **35**, 917 (1979).

[6] J. N. Bardsley and J. M. Wadehra, Phys. Rev. A **20**, 1398 (1979).

[7] J. M. Wadehra, Phys. Rev. A **29**, 106 (1984).

[8] C. Mündel, M. Berman, and W. Domcke, Phys. Rev. A **32**, 181 (1985).

[9] A. P. Hickman, Phys. Rev. A **43**, 3495 (1991).

[10] D. E. Atems and J. M. Wadehra, Chem. Phys. Lett. **197**, 525 (1992).

[11] D. E. Atems and J. M. Wadehra, J. Phys. B **26**, L759 (1993).

[12] P. L. Gertitschke and W. Domcke, Phys. Rev. A **47**, 1031 (1993).

[13] G. A. Gallup, Y. Xu, and I. I. Fabrikant, Phys. Rev. A **57**, 2596 (1998).

[14] Y. Xu and I. I. Fabrikant, Appl. Phys. Lett. **78**, 2598 (2001).

[15] A. Dalgarno and J. C. Browne, Astron. J. **149**, 231 (1967).

[16] J. C. Y. Chen and J. L. Peacher, Phys. Rev. **168**, 56 (1968).

[17] J. C. Browne and A. Dalgarno, J. Phys. B **2**, 885 (1969).

[18] R. J. Bieniek and A. Dalgarno, Astron. J. **228**, 635 (1979).

[19] K. Sakimoto, Chem. Phys. Lett. **164**, 294 (1989).

[20] M. Čížek, J. Horáček, and W. Domcke, J. Phys. B **31**, 2571 (1998).

[21] H. S. Taylor and F. E. Harris, J. Chem. Phys. **39**, 1012 (1963).

[22] J. N. Bardsley, A. Herzenberg, and F. Mandl, Planet. Space Sci. **89**, 305 (1966).

[23] J. C. Y. Chen and J. L. Peacher, Phys. Rev. **167**, 30 (1968).

[24] C. W. McCurdy and R. C. Mowrey, Phys. Rev. A **25**, 2529 (1982).

[25] M. Berman, C. Mündel, and W. Domcke, Phys. Rev. A **31**, 641 (1985).

[26] R. J. Bieniek, J. Phys. B **13**, 4405 (1980).

[27] V. I. Khvostenko and V. M. Dukel'skii, Sov. Phys. JETP **7**, 709 (1958).

[28] R. E. Hurley, Nuclear Instruments and Methods **118**, 307 (1974).

[29] W. Aberth, R. Schnitzer, and M. Anbar, Phys. Rev. Lett. **34**, 1600 (1975).

[30] J. Horáček, M. Čížek, K. Houfek, P. Kolorenč, and W. Domcke, Phys. Rev. A **70**, 052712 (2004).

[31] W. W. A. K. Belyaev, Y. Xu, A. Zhu, C. Xiao, and Xue-Feng Yang, Chem. Phys. Lett. **377**, 512 (2003).

[32] M. Čížek, J. Horáček, and W. Domcke, ECAMP in Rennes (2004), poster presentation.

[33] M. Čížek, ICPEAC in Rosario (2005), review talk.

[34] J. Horáček, M. Čížek, K. Houfek, P. Kolorenč, and W. Domcke, Phys. Rev. A **73**, 022701 (2006).

[35] M. Allan, J. Phys. B **18**, 451 (1985).

[36] M. Allan, M. Čížek, J. Horáček, and W. Domcke, J. Phys. B **33**, L209 (2000).

[37] H. Gnaser and R. Golser, Phys. Rev. A **73**, 021202(R) (2006).

[38] O. Heber, R. Golser, H. Gnaser, D. Berkovits, Y. Toker, M. Eritt, M. L. Rappaport, and D. Zajfman, Phys. Rev. A **73**, 060501(R) (2006).

[39] W. Domcke, Phys. Rep. **208**, 97 (1991).

[40] M. Čížek, J. Horáček, M. Allan, and W. Domcke, Czech. J. Phys. **52**, 1057 (2002).

[41] R. J. Bieniek, Phys. Rev. A **18**, 392 (1978).

[42] E. Narevicius and N. Moiseyev, Phys. Rev. Lett. **84**, 1681 (2000).

[43] S. A. Gurvitz, Phys. Rev. A **38**, 1747 (1988).

[44] W. Domcke, Phys. Rev. A **28**, 2777 (1983).

[45] J. Senekowitsch, P. Rosmus, W. Domcke, and H. J. Werner, Chem. Phys. Lett. **111**, 211 (1984).

[46] L. Pichl, Czech. J. Phys. **55**, 167 (2005).

[47] R. E. Hurley, Nucl. Instr. and Meth. in Phys. Research **118**, 307 (1974).

[48] W. Aberth, R. Schnitzer, and M. Anbar, Phys. Rev. Lett. **34**, 1600 (1975).

[49] Y. K. Bae, M. J. Coggiola, and J. R. Peterson, Phys. Rev. A **29**, 2888 (1984).

[50] At very large internuclear separation of about $R = 30\mathrm{a}_0$ the polarisation attraction between $\mathrm{H}+\mathrm{H}^-$ prevails. A shallow minimum is thus formed that may support 1-2 states with possibly large lifetimes. This possibility is not considered here.

[51] Previously [1], we had reported 14 μs as the longest lifetime for D_2^-. This result was flawed because of an numerical instability of the previous calculation for the narrowest resonances.